Mediterranean Arhaeology and Archaeometry, Vol. 12, No 2, pp.81-93

A TECHNICAL CHARACTERIZATION OF ROMAN PLASTERS, LUXOR TEMPLE, UPPER EGYPT

Hussein Marey Mahmoud [1*], Nikolaos Kantiranis[2], John Stratis[3]

[1]Department of Conservation, Faculty of Archaeology, Cairo University, Giza 12613, Egypt.
[2]Department of Mineralogy-Petrology-Economic Geology, Aristotle University, 54124 Thessaloniki, Greece.
[3] Laboratory of Analytical Chemistry, Aristotle University, 54124 Thessaloniki, Greece.

Received: 26/6/2011
Accepted: 15/3/2012
Corresponding autho Hussein Marey Mahmoudr: (marai79@hotmail.com)

ABSTRACT

The present paper aims to characterize some Roman plasters from the reign of the Emperor Diocletian in the late 3rd century AD. These plasters were applied over Pharaonic walls from the reign of Amenhotep III (c.1402–1364 BC) at Luxor temple, Upper Egypt. For the characterization of theses plasters, several analytical techniques were applied such as optical microscopy (OM), scanning electron mi-croscopy (SEM) equipped with an energy dispersive X-ray detector (EDS), X-ray powder diffraction analysis (XRPD), micro-Raman and Fourier transform infrared spectroscopies (μ-Raman and FT–IR). Based on the results of these analyses, the stratigraphic structure of the plaster layers was identified as fine coat '*intonaco*' which is based mainly on lime and coarse coat '*arriccio*' which consists of silica sand, phases of calcium carbonates and different pozzolanic additives. Moreover, the results revealed the green pigment as green earth (celadonite), the red pigment as red ochre, the yellow pigment as yellow ochre and the white pigment as calcium carbonate. The obtained data helped in improving our knowledge of some materials used during the Roman age in Egypt.

KEYWORDS: Roman plasters, Luxor temple, XRPD, SEM–EDS, μ-Raman, FT–IR

1. INTRODUCTION

Luxor temple is a famous and relatively complete Pharaonic temple located in the east bank of the River Nile, about 670km south of Cairo. Basically, Luxor temple was consecrated to Amon Ra in his fertility aspect. Amenhotep III (c.1386–1349) built Luxor temple on the site of a small temple of Amon, built by Kings of the 12th dynasty (c.1991–1786 BC). At the time of Amenhotep III, the temple was only 190 meter in length and 55 meter in width. In the 3rd century, the temple was converted into a fort, with a perimeter wall, from which the town derives its current name. There are scant remains of the fort itself, though some walls can be seen and a number of Roman brick columned structures give evidence of this period.

1.1 Historical context

During the reign of Diocletian, the 1st Maximian was one of two legions founded to defend Upper Egypt and was named for his colleague as Emperor, Maximianus. The legion was based at Luxor and converted one of the halls of the Luxor temple into a fortress. These legions were raised by Diocletian (AD 284–305) and it is that emperor whose image graces one of the walls of this room. This in turn became a church in the late Roman period. This area is also known as the Roman Sanctuary (Fig. 1) and it was a hypostyle hall occupied by eight columns which were removed when the area was converted into a Roman church (Kamil, 1976). The door to the Roman church was walled into a curved recess flanked by two granite Corinthian columns (Fig. 2a). Also, the reliefs on the walls were covered by plaster layers and painted with Christian scenes. In places where the plaster has fallen off, one can see Pharaonic reliefs of the time of Amenhotep III beneath (Fig. 2b,c). However, even if the Greeks were familiar with lime, they used it es-sentially only for stucco, painted render-ing and the lining of cisterns. The important contribution made by the Romans was the widespread use of lime for the manufacture of mortar to bond rubble masonry, replacing clay and thus achieving a permanent 'glue' which en-abled the use of concrete masonry in the most enormous constructions (Adam, 2005).

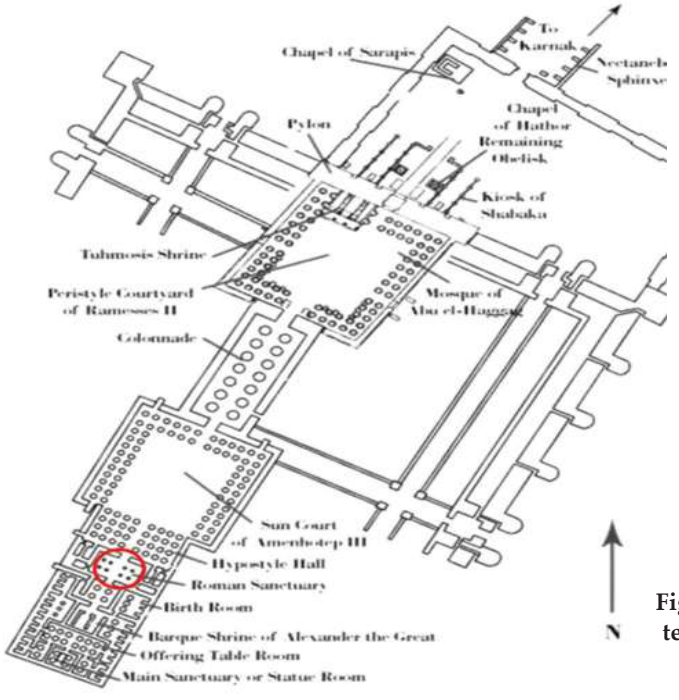

Figure 1: A general plan of Luxor temple, the Roman Sanctuary is highlighted with a cycle.

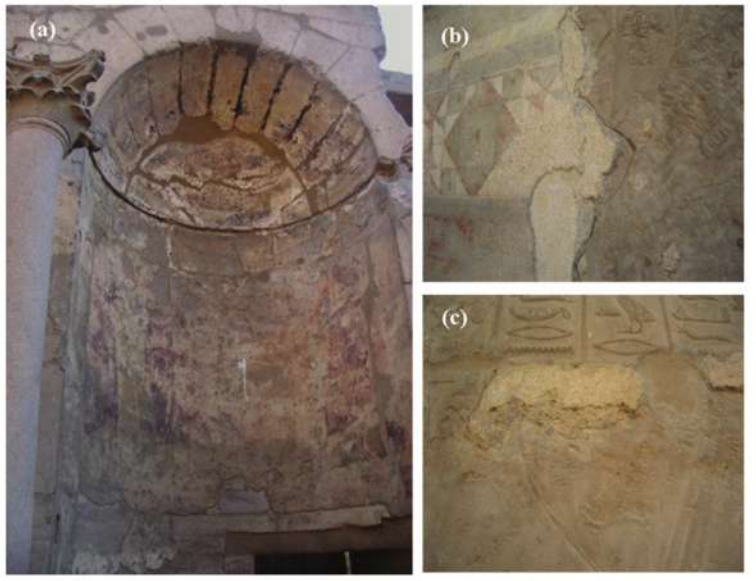

Figure 2: (a) The Roman church at Luxor temple; (b) Stratigraphic view of the Roman plasters; (c) The remains of the Roman plasters on the Pharaonic walls.

There are few original sources on Ro-man wall paintings; the only reference manuscripts are Pliny's *Naturalis historia, Vitruvius*' De architectura and Heraclius' *De coloribus et artibus Ro-manorum* (Baraldi et al., 2006). Roman wall paintings are applied either to dry lime plaster *(a secco)* or using *fresco* technique. The plaster supports are built up from several layers of lime plaster, with the uppermost containing a lime cement binder (Siddall, 2006). Vitruvius (1960) had recommended that seven successive layers of three different qualities made a good rendering: a first rough layer; three layers of mortar made with sand; then three layers of mortar made with powdered marble. In Roman monuments, the external and internal wall coverings are made up of three successive layers. The first rendering was made up of lime and unsifted sand, to maintain a certain roughness; its thickness, which varied considerably according to the nature and irregularity of the surface to be covered, was always considerable (approx. 3 to 5cm). The second coating, of a similar thickness or less (2 to 4cm), was done with a finer mortar made with sifted sand. The last layer, which could be as fine as one or two millimetres thick, was often made of pure lime that had been carefully thinned (Adam, 2005).

1.2 Research aims

In general, many studies have been de-voted to characterize materials from ob-jects dated back to the Roman age, such materials are wall paintings and pigments (Mirti et al., 1995; Bläuer-Böhm et al., 1996; Siddall, 2006; Aliatis et al., 2009), mortars (Velosa et al., 2007; Castriota et al., 2008; Franquelo et al., 2008; Duran et al., 2010), and painted plasters (Mazzocchin et al., 2004; Maz-zocchin et al., 2006; Mazzocchin et al., 2007; Mazzocchin et al., 2010; Baraldi et al., 2006). The study of Katsaros et al. (2011) revealed that the Theophrastus' "psimythion" and "kyanos egyptios" are attributed to the lead white (cerussite and hydrocerussite) and the Egyptian blue (cuprorivaite) respec-tively. Concerning

Egypt, few studies point out to identify materials from the Roman age in Egypt; some of these studies are the study of Ali (2003) on blue and green pigments from Greek-Roman objects in Egypt. Moreover, Berry (1999) studied pigments from a Roman shrine dated back to the 2nd century AD from the excavations of the town of Ismant El-Kharab, El Dakhleh Oasis. For this, the main research task was devoted to characterize some plasters collected from Roman plasters applied on the Pharaonic walls of Luxor temple. In this work, the analytical techniques utilized to study the plasters were: optical microscopy (OM), scanning electron microscopy (SEM) equipped with an energy dispersive X-ray detector (EDS), X-ray powder dif-fraction analysis (XRPD), micro-Raman and Fourier transform infrared spectroscopies (μ-Raman and FT–IR). The re-sults offered us more information about the stratigraphic structure and the chemical composition of these plasters.

2. MATERIALS AND METHODS

2.1. Samples

A total number of eighteen (18) tiny pieces of the plaster layers were carefully chosen from areas that seriously damaged in order to provide stratigraphic information of the paint layers. In areas showing a good state of con-servation, few powders of the pigments were carefully scrapped off using a microscalpel, beneath the pictorial layers.

2.2. Analytical techniques

2.2.1. Optical Investigation

In order to analyze the stratigraphy of the plaster layers, some samples were embedded in Epoxy resin (EpoFix), crosssectioned on variable speed silicon carbide papers, and examined using a Zeiss (stemi DV4) stereomicroscope with Sony (DSC−S85) camera. The size of the particle to be mounted should be as large as necessary, but as tiny as possible; usually, a particle with a size of 1x2 mm is absolutely sufficient and care should be taken that the sample contains all layers of multilayered paint.

2.2.2. Scanning electron microscopy (SEM–EDS)

In any case, the elemental microanalysis by SEM–EDX is always a valuable preliminary orientation (Franquelo et al., 2009). When analyses need to be performed within the bulk of a sample, the sample is often embedded in epoxy, ground and polished (Adriaens and Dowsett, 2004). In this study, the morphology of the plaster layers was investigated using a JEOL JSM-840A scanning electron microscope and the mi-croanalysis was carried out using an energy dispersive X-ray detector (EDS) Oxford ISIS 300 micro analytical sys-tem, with a detection limit of less than 1% depending on the element. The matrix correction protocol was ZAF correction (Z atomic number, A absorption, F fluorescence). In addition, polished cross-sections were investigated in the backscattered electrons mode (BSE).

2.2.3. X-ray powder diffraction analysis (XRPD)

XRD is indispensable in the identification of very rare pigments, minerals composed of widespread elements, such as bole grounds (earthy pigments of yellow or red colour) (Hradil et al., 2003). The collected samples were grounded into powder in an agate mortar and XRD measurements were performed using a Phillips PW1710 diffractometer with Ni-filtered Cu-kα radiation on randomly oriented samples. The samples were scanned over the 3−63º 2θ interval at a scanning speed of 1.2°/min. Quantitative estimates of the abundance of the mineral phases were derived from the XRD data,

using the intensity of a certain reflection, the density and the mass absorption coefficient for Cu-kα radiation for the minerals present. Corrections were made using external standard mixtures of minerals. The detection limit was ±2 % w/w.

2.2.4. μ-Raman spectroscopy

Raman spectroscopy probes molecular and crystal lattice vibrations and there-fore is sensitive to the composition, bonding, phase, and crystalline structure of the sample material. When Raman spectrometer is combined with the microscope, analysis is spatially refined, and by carrying out Raman measurements at various places of the sample (mapping the sample) it is possible to obtain detailed information regarding the distribution of specific compounds. Micro-Raman spectra were recorded us-ing a triple grating spectrometer (Dilor XY) equipped with a Charge Coupled Device (CCD) liquid-nitrogen cooled detector system. The red line (632.8 nm) spectra were excited from a 35 mW air-cooled He–Ne laser (Spectra Physics, mod.127). The spectral resolution of the system was ~3 cm^{-1}. The laser was focused on the sample through the system's microscope equipped with a standard objective lens 100x. In order to avoid dam aging of samples, the laser power was kept at 0.1–0.3mW.

2.2.5. Fourier transform infrared spec-troscopy (FT–IR)

Infrared spectroscopy in its traditional mode of transmittance is a powerful tool for analyzing both organic and inor-ganic materials, including crystalline and amorphous minerals. FT–IR spectra were collected using a Perkin-Elmer Spectrum One FT–IR Spectrometer on fresh KBr pellets of powdered samples were prepared and examined in trans-mittance mode in the range 4000–400 cm^{-1} at a resolution of 4 cm^{-1}.

3. RESULTS

3.1. Optical examination

Figure 3 shows stereomicroscopic im-ages obtained on polished cross-sections of the plaster layers. From the optical examination we can distinguish two plaster layers, the first one is in the bottom, the coarse plaster *'arriccio,'* its thickness ranges from 150 to 350 μm. This layer is based

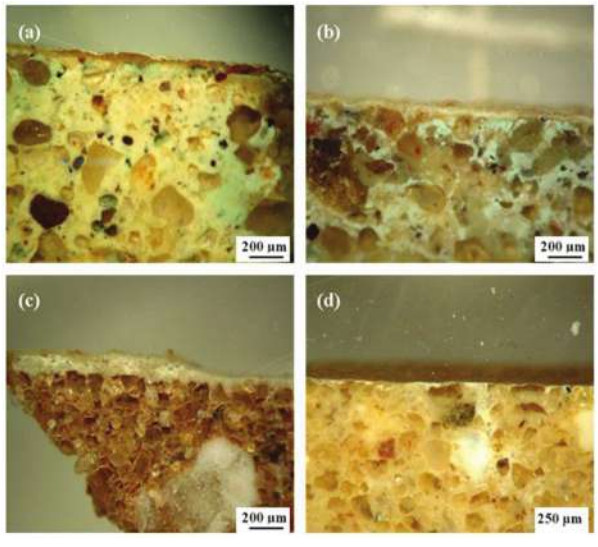

Figure 3: Stereomicroscopic photomicrographs show stratigraphic sections in the exam-ined plaster layers; (a) Details in the coarse plaster; large grains of silica sand and crushed ceramic are notable; (b) The thick coarse plaster in the bottom and the thin lime wash in the top; (c) Siliceous aggregates and voids are observed in the coarse plaster; (d) A close up shows the thin layer of the lime wash.

mainly on sand grains with different dimensions and colours embedded in the calcareous matrix (lime). Grains of crushed ceramic and bricks are also notable in this layer (Fig. 3a,b).

The second layer is in the top, the fine plaster *'intonaco'* is based mainly on a pure lime (as confirmed by XRPD analysis). The thickness of this layer is ranging from 50 to 150 μm (Fig. 3c,d).

3.2. SEM–EDS results

Table 1 shows the results of EDS microanalysis carried out on the studied samples. The SEM and BSE micro-graphs obtained on the outer surface of the fine plaster samples show small particles of calcium carbonate and grains of quartz are distributed in the calcareous matrix. EDS microanalysis of the sample shows a high proportion of calcium, which refers to calcium carbonates. Mi-nor amounts of silicon and aluminium were found, while traces of magnesium, iron and sodium were also detected. The silicon detected in the samples is due to fine siliceous aggregates of sand. EDS microanalysis of the coarse plaster shows silicon and calcium as major ions contained. SEM and BSE images obtained on the green pigment sample (Fig. 4a,b) show a thick massive paint layer with aggregates within the layer. Element concentration analysis by EDS ascertained that the green grains are green earth, since potassium, aluminium, silicon and iron were detected. Among mineral pigments, only green earth contains the above elements while the absence of Cu excludes the exis-tence of malachite or atacamite [$Cu_2Cl(OH)_3$]. Also, the absence of sodium suggests that celadonite was used to obtain the colour. From another location of the wall, a light green pigment was collected; the EDS microanalysis showed the absence of copper, while a high ratio of chromium (Cr) (wt. 28.83%) was detected. That probably suggests the use of modern paints of chromium oxide for retouching of the paintings. Chromium oxide is a dull, opaque, olive-green colour, identified by the chemical formula Cr_2O_3. Chromium oxide was referred to viridian when it was

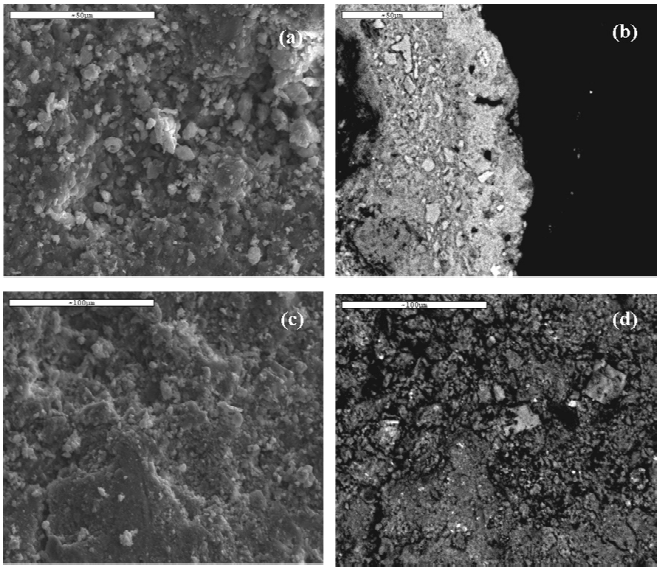

Figure 4: SEM and BSE micrographs obtained on some painted plaster layers. (a) SEM micrograph obtained on the outer surface of a green painted plaster shows the massive surface of the paint; (b) BSE micrograph obtained on a polished cross-section of the same sample shows the pigment grains are embedded in the lime matrix; (c) SEM micrograph obtained on the outer surface of a red painted plaster shows the coarse aggregates particles of the pigment material; (d) BSE micrograph obtained on the outer sur-face of the same sample shows fine grains of red ochre, with slightly large crystals of gypsum and the calcite ones are much smaller.

first discovered. The SEM and BSE images obtained on the red pigment sample (Fig. 4c,d) show granular coarse aggregates particles and large crystals of quartz distributing within the plaster layer. Small grains of gypsum are also notable.

On the other hand, a differentiation in the size between the grains of gypsum and calcite is easily observed, as the grains with gypsum are slightly large while the calcite

Table 1 EDS microanalysis (Atomic wt. %) of the studied samples

Sample/ Element	Na	Mg	A1	Si	S	Ca	K	Fe	Ti	Ba	Cr
Fine plaster	7.27	2.69	7.58	9.68	2.00	66.42	3.82	–	–	–	–
	3.85	1.97	6.09	15.79	7.79	59.67	–	–	2.86	1.98	–
	–	5.37	14.13	4.56	–	74.29	1.65	–	–	–	–
Coarse plaster	1.03	2.76	4.54	59.32	–	22.46	2.68	–	–	7.21	–
	1.32	1.66	8.28	55.34	–	27.32	3.21	–	2.87	–	–
	1.04	1.54	4.32	68.43	3.40	13.76	1.36	–	1.72	4.43	–
Green pigment	–	2.22	5.27	20.16	8.47	25.14	2.87	22.67	3.20	–	–
	–	4.87	6.54	32.43	–	13.25	2.43	16.11	2.76	–	–
	–	3.65	3.84	18.54	–	11.65	–	37.65	–	–	26.43
Red pigment											
	1.32	1.22	14.73	28.27	1.28	29.15	1.95	14.49	1.59	–	–
	–	1.69	9.09	35.91	–	30.25	1.76	19.53	1.77	–	–
	1.74	1.63	7.76	38.52	–	28.87	1.22	16.63	3.63	–	–
Yellow pigment	1.20	1.12	12.46	44.11	–	22.67	1.09	14.33	1.43	1.45	–
	0.89	1.19	11.16	38.72	11.43	18.83	2.42	12.73	1.53	098	–
	1.56	1.67	6.98	56.87	–	9.68	1.11	20.90	1.23	–	–
White pigment	1.08	2.64	2.54	10.38	2.76	78.54	1.62	–	–	–	–
	1.15	2.76	2.86	4.76	1.95	84.65	1.87	–	–	–	–
	1.74	1.98	5.76	12.76	1.82	74.87	1.07	–	–	–	–

ones are much smaller. EDS results show that silicon, calcium, sulphur and iron are the major ions contained. Elements of aluminium, potas-sium, and sodium were also measured.

The beak of iron suggests the use of iron oxides (probably hematite, Fe2O3) as colouring material. EDS microanalysis of the yellow pigment shows the detection of magnesium, aluminium, silicon, sulphur, potassium, calcium, titanium and iron. The peak for iron indicates the existence of iron oxide (probably goethite, FeOOH).

The contribution of silicon and aluminium indicates the presence of aluminosilicate materials. EDS microanalysis of the white pigment shows a high ratio of calcium with minor amounts of silica. Elements of aluminium,

potassium, and sodium, magnesium, sulphur were also measured.

3.3. Mineralogical characterization (XRPD)

The mineralogical characterization of the studied samples is given in Table 2. XRPD analysis of the fine plaster indicated calcium carbonate (calcite, $CaCO_3$) as the predominant phase in the sample. Traces of quartz (SiO_2) and plagioclase (albite, $NaAlSi_3O_8$) were also measured. XRPD analysis of the coarse plaster indicated the presence of quartz as the main component; among the minor components are K-feldspar, calcite (rhombohedral $CaCO_3$), vaterite (a rare hexagonal polymorph of $CaCO_3$) and plagioclase. Traces of gypsum ($CaSO_4 \cdot 2H_2O$), amphibole (tremolite), barite ($BaSO_4$), and mica (muscovite) were also measured. XRPD analysis of the red pigment showed that quartz is the main component, with minor amounts of calcite. Traces of hematite, plagioclase, gypsum and clay minerals were also detected. XRPD analysis of the yellow pigment showed calcite and quartz as the main component. Traces of goethite, Kfeldspar and clay minerals were also found. XRPD analysis of the white pigment showed that calcite is the main component, while traces of quartz were also found.

3.4. FT–IR results

An FT–IR spectrum recorded on a KBr disk of the fine plaster (Fig. 5a) shows that vaterite gives only one absorption at 1470.93 cm^{-1} due to the CO^{2-} asymmetrical stretching (v3), while other absorptions at

Table 2 The mineralogical composition of the studied samples

Sample/ Component	*C*	*Q*	*V*	*Kf*	*Pl*	*He*	*Go*	*Cl*	*Ba*	*Am*	*Gy*	*M*
Fine plaster	+++	+	–	–	+	–	–	–	–	–	–	–
Coarse plaster	–	+++	++	++	+	–	–	+	+	+	+	+
Red pigment	++	+++	–	–	+	+	–	+	–	–	+	–
Yellow pigment	+++	+++	–	+	–	–	+	+	–	–	–	–
White pigment	+++	+	–	–	–	–	–	–	–	–	–	–

C= calcite; Q=quartz; V= vaterite; Kf= potassium feldspar; Pl= plagioclase; He= hematite; Go= goethite; Cl=clay minerals; Ba= barite; Am=amphibole, Gy= gypsum; M=Micas. – = not determined; + = traces; ++ = minor constituent; +++ = major constituent.

876.11 cm^{-1} probably assigned to amorphous calcium carbonate and at 746.85 cm^{-1} (in plane bending, v4). In this case, the vl vibration around 1089.56 cm^{-1} was detectable. The band at 461.92 cm^{-1} indicates amorphous silicates probably come from the ceramic fragments contained in the mortar.

The FT–IR spectrum recorded on the green pigment show the following bands

arise at: 3569.39 and 3395.25 cm^{-1} (O–H stretching), 1166.23 cm^{-1} (Si–O vibration perpendicular to SiO_4 tetrahedral sheet), 1087.07 and 1004.75 cm^{-1} (in-plane Si–O stretching modes) (Ospitali et al., 2008). The band at 799.95, 680 cm^{-1} (R–O–H bending, where R is the octahedral ion $^{-}$Al, Fe^{+2}, Fe^{+3}, Mg). These bands are attributed to green earth and specifically to cela-donite (Zorba et al., 2006). The bands at 2929.82 and 2853.83 cm^{-1} (v_{asym} and $v_{sym}CH_2$), probably due to the presence of polyvinyl acetate used as a modern coating varnish, the bands at 1419.53 and 871.17 cm^{-1} are related to calcium carbonate, while the bands at 1615.83 and 779.95 cm^{-1} are related to calcium sulphates. FT–IR spectrum collected on the yellow pigment show bands at 797 and 902 cm^{-1} are assigned to the vibrational modes of goethite. These are distinguishable but, for painting samples in which mixtures of compounds are very common, it is sometimes difficult to differentiate them from the corresponding ones for stretching Si–O situated in the range 900–1100 cm^{-1}, if they are accompanied of silicates (ochres) (Fran-quelo et al., 2009). The band at 1452.68 cm^{-1} is attributed to calcite, and the band at 1629.67 cm^{-1} is attributed to gypsum. The bands at 1083.46 and 1032.33 cm^{-1} are attributed to (Si–O) stretching; the bands at ~411 and 463.23 cm^{-1} indicate the presence of amorphous silica. The band at ~3430 cm^{-1} is due to free hydroxyl ions of kao-linite, peaks of water H–O–H str., and a broad peak at~3140 cm^{-1} which was attributed to the peak of hydrated ferric oxide.

3.5. μ-Raman results

Micro-Raman spectroscopy was used as a complementary technique to study some pigments. A μ-Raman spectrum recorded on the red pigment (Fig. 5b) shows the characteristic bands at ~226, 298 and 408 cm^{-1} are attributed to hematite. μ-Raman spectra recorded on the yellow pigment show the bands at ~247, 280, 302, 386, 460 and 506 cm^{-1} were recorded, which refers to goethite.

4. DISCUSSION

4.1. Plaster layers

The results of the XRPD and FT–IR analyses indicate that calcite is the main component of the studied plasters. The fine plaster *'intonaco'* is based mainly on lime. The second layer *'arriccio'* is slightly thick and was prepared from lime and large grains of silica sand. XRD measurements of this layer showed that it consists of quartz, K-feldspar, two phases of calcium carbonate (calcite & vaterite), gypsum, amphi-bole, barite and plagioclase. FT–IR analysis indicated the existence of amorphous silica in the studied samples, which probably resulted from the poz-zolanic additives to the plasters. According to Velosa et al. (2007), crushed ceramic particles were employed in Roman mortars for the purpose of creat-ing pozzolanic reactions between the finer particles and lime. he microanalysis of the studied samples showed the presence of major amounts of $CaO–SiO_2$, with minor amounts of Al_2O_3, MgO, Fe_2O_3 and K_2O.

This suggests that a hydraulic lime. The hydraulic compounds are obtained from the reactions of $Ca(OH)_2$ with natural pozzolanes (natural earth of volcanic source) or artificial ones (such as ground fired bricks and tiles or ceramic shreds) (Franquelo *et al.* 2008).

4.2. Green pigment

The green pigment in the examined plasters was identified as green earth. The predominant green pigments in Roman wall paintings are green earths (Bearat and Pradell, 1997). Green earth is described as a clay pigment with a chromogenous element in the clay structure, generally a hydrated alumi-nosilicate of magnesium, iron and potassium (Genestar and Bonafé, 2004). The primary source minerals for the pigment

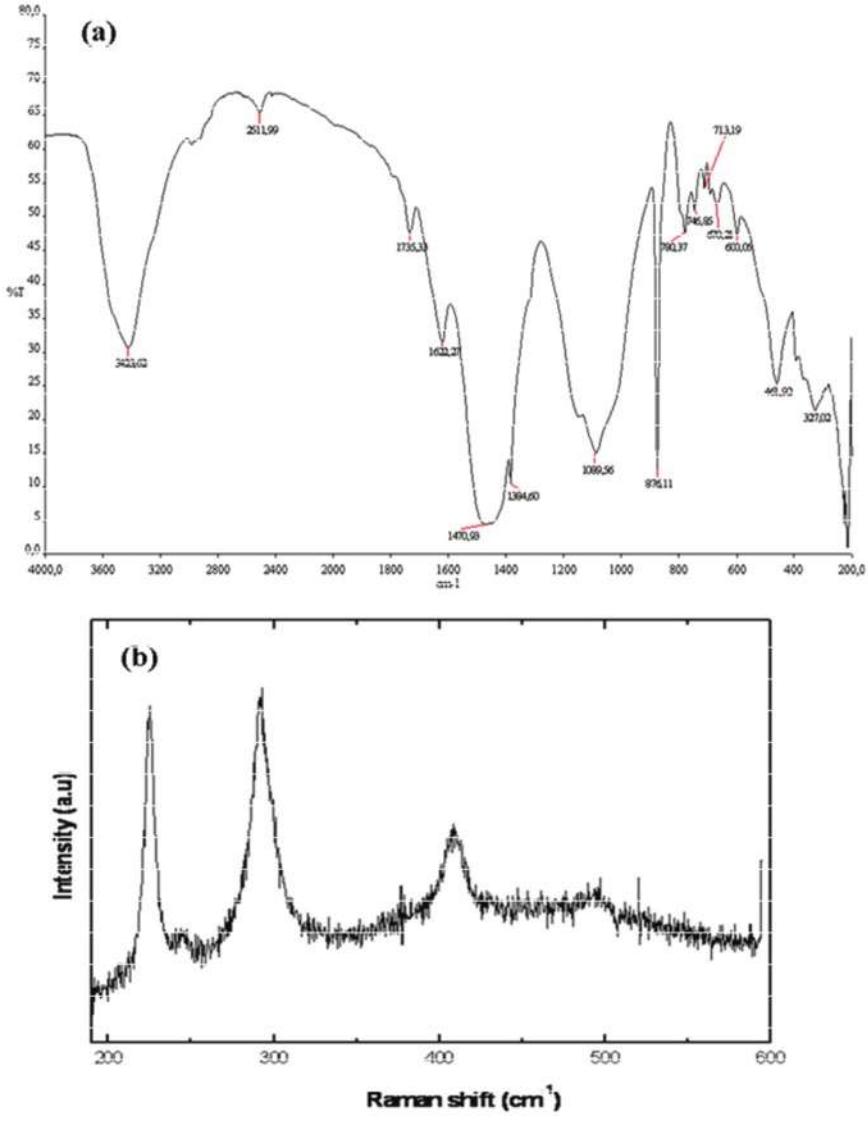

Figure 5: (a) an FT–IR spectrum obtained on the fine plaster layer; (b) μ-Raman spectrum obtained on the red pigment.

known as green earth are the dioctahedral micas, celadonite and glauconite (Wainwright et al., 2009). These two minerals are hardly distinguishable and most authors do not differentiate the phases, simply calling the material "green earth" (Aliatis et al., 2009; Ospitali et al., 2008). The colour of celadonite has been described as earthy, dull, greygreen or bluish-green. The chemical composition of celadonite is approximately K [(Al, Fe^{3+}),(Fe^{2+}, Mg)] ($AlSi_3$, Si_4)$O_{10}(OH)_2$ with low aluminium content and a very small replacement of Al for Si in the tetrahedral layer (Aliatis et al., 2009).

4.3. Red pigment

Red ochre was identified as red pigment in the studied plasters. Red ochre was used from the 5th Dynasty till the Roman times (Lee and Quirke, 2000). The actual pigments

are hematite, an iron (III)-oxide (Bikiaris et al., 1999; Casel-lato et al., 2000; Ortega et al., 2001). Well-crystalline hematite has a distinct violet tint differing from the bright red colour of, e.g. pedogenic. The poorly crystallized hematite was associated with quartz, plagioclase, potassium feldspar and illite.

4.4. Yellow pigment

Yellow ochre was widely used without interruptions from the 5th Dynasty (c.2494-2345 BC) till the Roman period in Egypt (El Goresy et al., 1986). The hue of goethite is affected by its crystallinity and elemental purity. Finely particulate (poorly crystalline) goethite, commonly called limonite in the past, is brownish yellow. Goethite only uniquely occurs in nature in a pure form or as a massive mineral (Ortega et al., 2001; Hradil et al., 2003).

4.5. White pigment

Calcite is one of the most common minerals on the face of the Earth. Calcium carbonates enjoyed wide application in ancient Egyptian decorations from the 5th Dynasty until the reign of the emperor Tiberius (El Goresy, 2000). The ancient Egyptians either used calcite senso stricto or chalk, and it is unknown if they used natural carbonates or decarbonated chalk (El Goresy et al., 1986).

5. CONCLUSIONS

In this work, different analytical techniques (OM, SEM–EDS, XRPD, μ-Raman and FT–IR) were employed to study Roman plasters at Luxor temple. The results showed that the plaster layers are based mainly on lime. Pozzolanic additives such as ceramic frag-ments were used to improve the durability of the plasters. The results indicated that calcite is the main component of the fine *'intonaco'* plaster. The coarse *'ar*riccio' plaster consists mainly of silica sand and phases of calcium carbonates. According to EDS, FT–IR and μ-Raman analyses, the green pigment was identified as green earth (compatible with celadonite), the red pigment as red ochre, the yellow pigment as yellow ochre and the white pigment as calcium carbonate. Restorations in recent times are suggested by the detection of chromium oxide (viridian) used for re-touching purpose. Moreover, the detection of polyvinyl acetate (PVAc) indicates recent restoration attempts of the murals. Further analysis on additional samples from the Roman age in Egypt will help in drawing a clear image about materials used in this era of the Egyptian history.

ACKNOWLEDGEMENTS

The authors are grateful to Mr. S. Oikonomidis, School of Geology, Aristotle University for his support through the SEM study. Special thanks are due to Mr. S. Haralampos and to Mr. Th. Dimitriadis, Department of Inorganic Chemistry, Aristotle University for their assistance in the study using FT-IR spectroscopy.

REFERENCES

Adam, J-P (2005) *Roman Building: Materials and Techniques,* Translated by Anthony Mathews, Taylor & Francis e-Library.

Adriaens, A., and Dowsett, M.G. (2004) Electron microscopy and its role in cultural heritage stuies. In: Janssens, K and Van Grieken, R. (Eds.), *Comprehensive Ana-lytical Chemistry, Vol. XLII "Non-destructive Microanalysis of Cultural Heritage Materials,* Elsevier, 73–124.

Aliatis, I., Bersani, D., Campani, E., Casoli, A., Lottici, P.P., Mantovan, A., Marino, I-G., Ospitali, F. (2009) Green pigments of the Pompeian artists' palette, *Spectrochimica Acta A,* Vol. 73, 532–538.

Ali, M.F. (2003) Comparison study of Blue and green pigments from the third intermediate period till the Greek Roman Period, *Egyptian Journal of Analytical Chemistry,* Vol.12, 21–30

Baraldi, P., Bonazzi, A., Gioedani, N., Paccagnella, F., and Zannini, P. (2006) Analytical characterization of Roman plasters of the *'Domus Farini'* in Modena, *Archaeometry,* Vol. 48, 481–99.

Bearat, H., and Pradell, T. (1997) Contribution of Mössbauer Spectroscopy to the study of Ancient Pigments and Paintings. In: Béarat, H., Fuchs, M., Maggetti, M and Paunier, D. (Eds.), *Roman Wall Painting: materials, techniques, analysis and conservation, Proceedings of the International Workshop,* Fribourg, Institute of Mineralogy and Petrography, University of Fribourg, 239–256.

Berry, M (1999) A study of pigments from a Roman Egyptian shrine, *AICCM Bulletin,* 1–9.

Bikiaris, D., Daniilia Sr., Sotiropoulou, S., Katsimbiri, O., Pavlidou, E., Moutsatsou, A.P., Chryssoulakis, Y. (1999) Ochre differentiation through micro-Raman and micro-FTIR Spectroscopes: application on wall paintings at Meteora and Mount Athos, Greece, *Spectrochimica Acta A,* Vol. 56, 3–18.

Bläuer-Böhm, Ch., and Jägers, E. (1996) Analysis and recognition of dolomitic lime mortars, in *Proceedings of the International Workshop on Roman Wall Painting, Roman Wall Painting Materials, Techniques, Analysis and Conservation, Fribourg, March 7–9, 1996* (eds. H. Béarat, M. Fuchs, M. Maggetti and D. Paunier), 223–35, Institute of Mineralogy and Petrology, Fribourg University.

Casellato, U., Vigato, P.A., Russo, U., Matteini, M. (2000) A Mössbauer Approach to the Physico-Chemical Characterization of Iron-Containing Pigments for Historical Wall Paintings, *Journal of Cultural Heritage,* Vol. 1, 217–232.

Castriota, M., Cosco, V., Barone, T., De Santo, G., Carafa, P., and Cazzanelli, E. (2008) Micro-Raman characterizations of Pompei's mortars, *Journal of Raman Spectroscopy,* Vol. 39(2), 295–301.

Duran, A., Jimenez De Haro, M. C., Perez-Rodriguez, J. L., Franquelo, M. L., Herrera, L. K., and Justo, A. (2010) Determination of pigments and binders in Pompeian paintings using synchrotron radiation – high-resolution X-ray power diffraction and conventional spectroscopy–chromatography, *Archaeometry*, Vol. 52, 286–307.

El Goresy, A., Jaksch, H., Abdel Razek, M., Weiner, K.L. (1986) Ancient pigments in wall paintings of Egyptian tombs and temples: an archaeometric project, Preprint of the Max Planck Institute of Nuclear Physics MPI H- V 12, Heidelberg.

El Goresy, A. (2000) Polychromatic Wall Painting Decorations in Monuments of Pharaonic Egypt: compositions, chronology and painting techniques, *Proceedings of the First International Symposium: "The Wall Paintings of Thera"*, Sherratt, S. (ed.), Vol. I, Petros M. Nomikos and Thera Foundation, Piraeus, Athens, Hellas, 49–70.

Franquelo, M. L., Robador, M. D., Ramírez-Valle, V., Durán, A., Jiménez de Haro, M. C., and Pérez-Rodríguez, J. L. (2008) Roman ceramics of hydraulic mortars used to build the Mithraeum house of Mérida (Spain), *Journal of Thermal Analysis and Calorimetry,* Vol. 92 (1), 331–5.

Franquelo, M.L., Duran, A., Herrera, L.K., Jimenez de Haro, M.C., Perez- Rodriguez, J.L. (2009) Comparison between micro-Raman and micro-FTIR spectroscopy techniques for the characterization of pigments from Southern Spain Cultural

Heritage, *Journal of Molecular Structure,* Vol. 924-926, 404–412.
Genestar, J.C., Bonafé, C.P. (2004) The use of natural earths in picture: study and differentiation by thermal analysis, *Thermochimica Acta,* Vol. 413, 185–192.
Hradil, D. Grygar T., Hradilova, J. Bezdička, P. (2003) Clay and iron oxide pigments in the history of painting, *Applied Clay Science,* Vol. 22, 223–236
Kamil, J (1976) LUXOR: *A Guide to Ancient Thebes,* (2nd ed.), London.
Katsaros, T, Liritzis, I and Laskaris, N (2011) Identification of Theophrastus' pigments egyptios kyanos and psimythion from archaeological excavations: A case study. *Archaeosciences (Revue d'Archaeometrie)* 34, 69–80.
Lee, L., Quirke, S (2001) Painting materials. In: Nicholson, T.P and Shaw, I. (Eds.), *Ancient Egyptian materials and Technology,* UK, 104–119.
Mazzocchin, G. A., Agnoli, F., and Salvadori, M. (2004), Analysis of Roman age wall paintings, *Talanta*, Vol. 64, 732–741.
Mazzocchin, G. A., Orsega, E. F., Baraldi, P., and Zannini, P. (2006) Aragonite in Roman wall paintings of the VIIIa Regio, Aemilia, and Xa Regio, Venetia Et Histria, *An*nali di Chimica, Vol. 96 (7–8), 377–387.
Mazzocchin, G. A., Del Faveroi, M., and Tasca, G. (2007) Analysis of pigments from Roman wall paintings in the 'Agro Centuriato' of Julia Concordia (Italy), *Annali di Chimica,* Vol. 97, 905–913.
Mazzocchin, G. A., Vianello, A., Minghelli, S., and Rudello, D. (2010) Analysis of Roman wall paintings from the Thermae of 'Iulia Concordia', *Archaeometry*, Vol. 52, 644–655.
Mirti, P., Appolonia, L., Casoli, A., Ferrari, R.P., Lurenti, E., Amisano Canesi, A., Chiari, G. (1995) Spectrochemical and Structural Studies on a Roman Sample of Egyp-tian blue, *Spectrochimica Acta A,* Vol. 51 (3), 437–446.
Ortega, M., Ascencio, J.A., San-Germán, C.M., Fernándes, M.E. (2001) Analysis of Prehistoric Pigments from "Templo Mayor" of Mexico City, *Journal of Materials Science*, Vol. 36, 751–756.
Ospitali, F., Bersani, D., Di Lonardo, G., Lottici, P.P.(2008) 'Green earths': vibrational and elemental characterization of glauconites, celadonites and historical pigments, *Journal of Raman Spectroscopy,* Vol. 39, 1066–1073.
Siddall, R. (2006) Not a day without a line drawn: Pigments and painting techniques of Roman Artists, *Infocus magazine, Proceedings of the Royal Microscopy Society,* issue 2, 19–31.
Velosa, L.A, Coroado, J., Veiga, R.M., Rocha, F. (2007) Characterisation of roman mortars from Conímbriga with respect to their repair, *Materials Characterization,* Vol. 58 (11-12), 1208–1216.
Vitruvius (1960) *The ten books on architecture VII,* transl. N. H. Morgan, 1st THUS edn, Dover Publications, NewYork
Wainwright, I.N.M., Moffatt, E.A., Sirois, P.J. (2009) Occurrences of green earth pig-ments on northwest coast first nations painted objects, *Archaeometry*, Vol. 51, 440–456.
Zorba, T., Pavlidou, E., Stanojlovic, M., Bikiaris, D., Paraskevopoulos, K.M., Nikolic, V., Nikolic, P.M. (2006) Technique and palette of XIIIth century painting in the monastery of Mileseva, *Applied Physics A,* Vol. 83, 719–725.